BIOCHEMISTRY

 Volume 44, Number 26 July 5, 2005

Accelerated Publications

Protein Dynamics in Living Cells†

Julie E. Bryant,‡ Juliette T. J. Lecomte,§ Andrew L. Lee,||,⊥,@ Gregory B. Young,⊥ and Gary J. Pielak*,‡,⊥,@

Departments of Chemistry and of Biochemistry and Biophysics, Division of Medicinal Chemistry and Natural Products, and Lineberger Cancer Research Center, University of North Carolina, Chapel Hill, North Carolina 27599, and Department of Chemistry, The Pennsylvania State University, University Park, Pennsylvania 16802

Received April 28, 2005; Revised Manuscript Received May 27, 2005

ABSTRACT: A protein's structure is most often used to explain its function, but function also depends on dynamics. To date, protein dynamics have been studied only in vitro under dilute solution conditions where solute concentrations are typically less than 10 g/L, yet proteins function in a crowded environment where the solute concentration can exceed 400 g/L. Does the intracellular environment affect protein dynamics? The answer will help in assessing the biological significance of the NMR-derived dynamics data collected to date. We investigated fast protein dynamics inside living *Escherichia coli* by using in-cell NMR. The backbone dynamics of apocytochrome b_5 were quantified using $\{^1H\}-^{15}N$ nuclear Overhauser effect (nOe) measurements, which characterize motions on the pico- to nanosecond time scale. The overall trend of backbone dynamics remains the same in cells. Some of the nOe values differ, but most of the differences track the increased intracellular viscosity rather than a change in dynamics. Therefore, it appears that dilute solution steady-state $\{^1H\}-^{15}N$ nOe measurements provide biologically relevant information about pico- to nanosecond backbone motion in proteins.

Understanding protein dynamics is critical to understanding the motions that allow proteins to function. Motions on the pico- to nanosecond time scale provide key information about the ensemble of protein conformations present under a given set of conditions (*1*). Protein backbone motions can be quantified using nuclear magnetic resonance spectroscopy (NMR)[1] by making ^{15}N relaxation measurements. Specifically, steady-state $\{^1H\}-^{15}N$ nuclear Overhauser effect (nOe) measurements provide information about the pico- to nanosecond time scale motions experienced by individual backbone amide ^{15}N nuclei (*2*). To date, ^{15}N relaxation studies have been carried out in vitro in dilute solution with solute concentrations typically around 10 g/L. Most proteins, however, carry out their biological functions under crowded conditions in vivo where the concentration of macromolecular species can reach greater than 400 g/L (*3*).

Theory and practice show that a crowded environment can affect biological processes, including protein−protein interactions (*4*), protein folding (*5*), protein aggregation (*6*), and

† This work was supported by the NSF (Grant MCB 0212939 to G.J.P.) and the NIH (Grant GM-54217 to J.T.J.L.). J.E.B. was partially supported by a Dobbins Fellowship.

* To whom correspondence should be addressed: Department of Chemistry, University of North Carolina, Chapel Hill, NC 27599. Phone: (919) 966-3671. Fax: (919) 966-3675. E-mail: gary_pielak@unc.edu.

‡ Department of Chemistry, University of North Carolina.

§ The Pennsylvania State University.

|| Division of Medicinal Chemistry and Natural Products, University of North Carolina.

⊥ Department of Biochemistry and Biophysics, University of North Carolina.

@ Lineberger Cancer Research Center, University of North Carolina.

[1] Abbreviations: NMR, nuclear magnetic resonance spectroscopy; nOe, nuclear Overhauser effect; HSQC, heteronuclear single-quantum coherence.

10.1021/bi050786j CCC: $30.25
Published on Web 06/10/2005

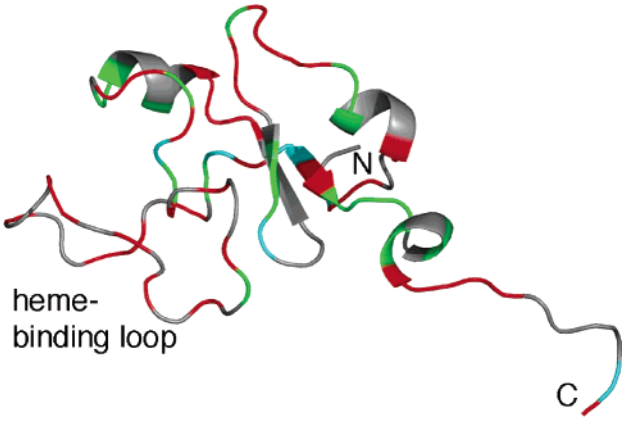

FIGURE 1: NMR structure of apocytochrome b_5 in dilute solution (*9*). Colors indicate increases (cyan), decreases (red), and no change (green) in $\{^1H\}-^{15}N$ nOe values in cells compared to the values in dilute solution (gray, no data). The first four residues are not observed in the solution structure.

protein stability (*7*). Does the intracellular environment affect fast backbone dynamics? The answer will help in assessing the biological significance of the vast amount of NMR-derived protein dynamics data collected to date. Here we assess fast protein dynamics in living cells with a new technique, in-cell NMR.

We chose the apo form of the water-soluble domain of rat microsomal cytochrome b_5, a small, soluble, and well-characterized protein with both rigid and highly dynamic regions (*8*). In dilute solution, the apo form of this 98-residue, 11.2 kDa electron transport protein exhibits reduced structure and increased backbone dynamics because it lacks a heme moiety (*8*). In Figure 1, the lack of highly defined tertiary structure in the heme-binding region and both termini is represented in the averaged NMR structure (*9*) by stringlike segments.

In-cell NMR allows for the investigation of proteins inside living *Escherichia coli* (*10*). Until now, this technique has mostly been used for qualitative analysis (*5*, *10*−*14*). Our goal is to develop this technique so it will yield quantitative information. In this work, the quantitative assessment of pico- to nanosecond protein backbone dynamics in living *E. coli* is achieved with in-cell NMR. First, we investigate the structure of apocytochrome b_5 in dilute solution and in living cells. Then, we measure the backbone amide $\{^1H\}-^{15}N$ nOe under both conditions and interpret the differences in terms of changes in fast protein dynamics and viscosity inside the cell.

EXPERIMENTAL PROCEDURES

In-Cell NMR Samples. The expression system for cytochrome b_5, pET3d(*cytb5*), is described elsewhere (*15*). The plasmid was transformed into *E. coli* strain BL21(DE3) Gold (Stratagene). Twenty-five milliliters of saturated overnight culture was used to inoculate 225 mL of ^{15}N-enriched Martek 9-N medium (Spectra Stable Isotopes) supplemented with ampicillin (100 μg/mL). After incubation for 2 h at 37 °C with shaking, cytochrome b_5 expression was induced with 1 mM (final concentration) isopropyl β-D-thiogalactopyranoside. The induced cells were harvested after 4 h by gentle centrifugation at ~1600*g* and 4 °C for 30 min. The system produces mostly the apoprotein, although the cell pellets are slightly pink, as reported previously (*15*). The supernatant was decanted and saved. Gentle agitation with 1.0 mL of this ice-cold spent medium was used to resuspend the cells. A sample of 90% cell slurry and 10% ^2H_2O (99.9% ^2H) was used. As shown by plating (see below), the cell concentration in the NMR sample is $\sim 2 \times 10^8$ cells/mL. A reference sample, for shimming the spectrometer before inserting the in-cell sample, was prepared from 90% spent medium and 10% ^2H_2O. In-cell samples were stored on ice prior to insertion into the spectrometer. The NMR experiments were started within 1 h of the cells being harvested.

Protein Purification. Apocytochrome b_5 was purified as described elsewhere (*15*) with a few modifications. Briefly, thawed cell pellets from in-cell NMR experiments were resuspended in a minimal volume of preparation buffer [50 mM tris(hydroxymethyl)aminomethane hydrochloride and 1 mM ethylenediaminetetraacetic acid (pH 7.5)] supplemented with 0.4 mM (final concentration) phenylmethanesulfonyl fluoride. The cells were lysed by repeated sonication on ice using a 10% duty cycle. The lysate was cleared by centrifugation at ~29000*g* and 4 °C for 45 min.

Chromatography was performed on an ÄKTA FPLC system (Amersham Biosciences) at 4 °C. The cleared lysate was applied to an anion exchange chromatography column (HiLoad 16/10 Q Sepharose High Performance, Amersham Biosciences). Unbound material was eluted with 2 column volumes of preparation buffer. Cytochrome b_5 (holo and apo) was eluted with the same buffer by using a linear gradient from 0 to 0.4 M NaCl over 20 column volumes. Fractions with significant absorbance at 280 nm were visualized after SDS−PAGE by staining with Coomassie Brilliant Blue. Fractions containing only apocytochrome b_5 (negligible absorbance in the visible region) were pooled and subjected to size exclusion chromatography (Superose 12 10/300 GL Tricorn High Performance, Amersham Biosciences) and eluted with 0.05 M ionic strength phosphate buffer (pH 7.0). Pure apocytochrome b_5 was dialyzed against this same buffer and concentrated to ~0.5 mM. Molecular weight analysis was performed on an aliquot of the in vitro NMR sample of apocytochrome b_5 in the Michael Hooker Proteomics Core Facility at the University of North Carolina. The calculated and observed molecular mass for the ^{15}N-enriched protein is 11 345 Da.

In Vitro NMR Samples. Pure ^{15}N-enriched apocytochrome b_5 (~0.5 mM) in phosphate buffer (pH 7.0) was used for dilute solution experiments with 10% ^2H_2O.

NMR. Experiments were conducted at 25 °C on Varian Unity Inova spectrometers equipped with 5 mm ^1H $\{^{13}C/^{15}N\}$ X, Y, Z PFG triple-resonance probes with three-axis gradients at The University of North Carolina Biomolecular NMR Laboratory. Data were processed with NMRPipe and analyzed with NMRDraw (*16*).

The in-cell $^1H-^{15}N$ heteronuclear single-quantum coherence (HSQC) (*17*, *18*) spectrum of apocytochrome b_5 was acquired at a ^1H frequency of 500.213 MHz with a ^1H spectral width of 6999.738 Hz and a ^{15}N spectral width of 2100.0 Hz. The number of complex points collected in t_2 was 1024. One hundred sixty increments of 156 transients each were acquired. The acquisition required approximately 15 h.

The in vitro $^1H-^{15}N$ HSQC spectrum was acquired at a ^1H frequency of 699.777 MHz with a ^1H spectral width of

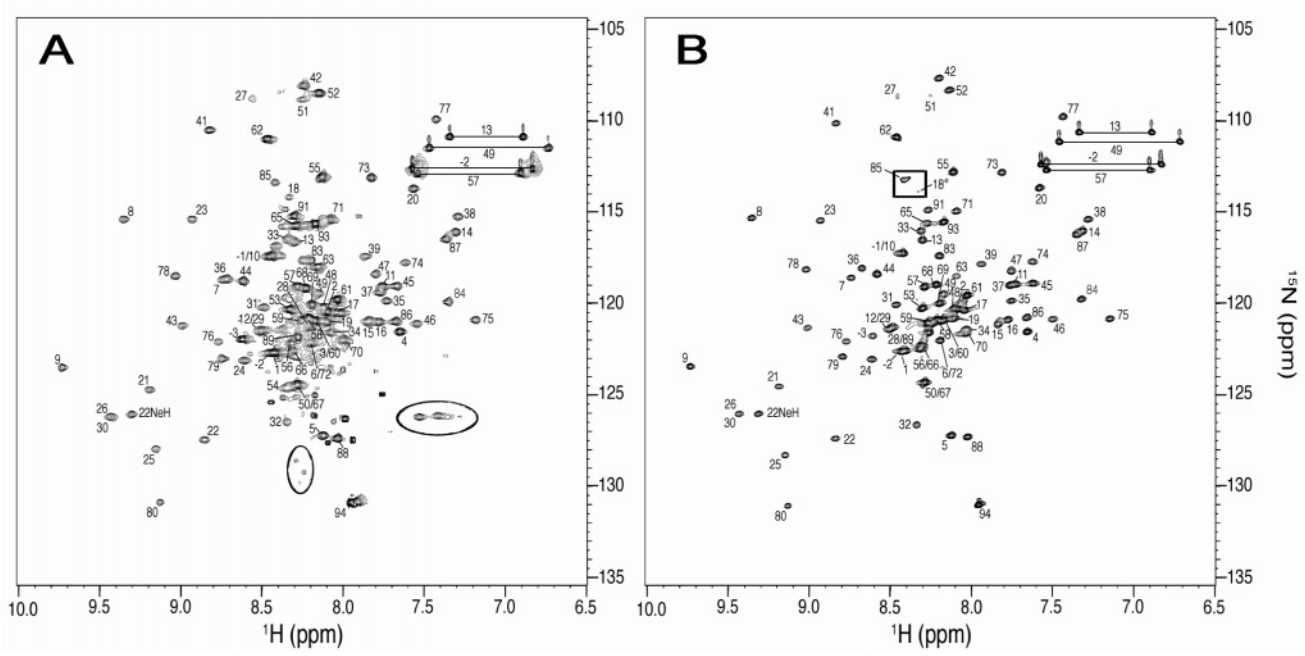

FIGURE 2: Apocytochrome b_5 ^{1}H−^{15}N HSQC spectra obtained in *E. coli* (A) and in dilute solution (B). Assignments are based on published values (*8*, *15*). ^{15}N-enriched cellular metabolites are circled in the in-cell spectrum. Cross-peaks for Ser18 and Ser85 are not visible in the dilute solution spectrum because of their lower intensity. These cross-peaks are visible at a lower contour level, as shown in the box.

11 422.209 Hz and a ^{15}N spectral width of 2187.6 Hz. The number of complex points collected in t_2 was 1024. One hundred fifty increments of 146 transients each were acquired. The acquisition required approximately 15 h.

The {^{1}H}−^{15}N steady-state nOe experiments were performed as described elsewhere (*19*, *20*). Briefly, each experiment consisted of two spectra, a reference spectrum and a nOe spectrum. Both spectra were acquired in identical fashion except that the nOe spectrum was acquired with a ^{1}H irradiation period of 4.5 s during the recycle delay to produce the steady-state nOe. The reference spectrum was acquired without ^{1}H saturation. The two spectra were acquired in an interleaved fashion at a ^{1}H frequency of 699.777 MHz with a ^{1}H spectral width of 9800.32 Hz and a ^{15}N spectral width of 2372.76 Hz. Each experiment comprised 512 complex points. Each of the 124 increments comprised 64 transients with a recycle delay of 5 s. The total acquisition time was ~45 h.

Controls. In-cell NMR samples were collected, fractionated into the soluble and insoluble portions of the extracellular and intracellular components of the sample, and subjected to SDS−PAGE. Proteins were visualized with Coomassie Brilliant Blue to ensure that the apocytochrome b_5 was located in the soluble cytoplasmic fraction of the cells during acquisition of the spectrum. The viability of the cells was quantified by triplicate serial dilution of aliquots before and after a 48 h experiment. Samples were plated on Luria broth plates supplemented with ampicillin (100 μg/mL). Colonies were counted after incubation overnight at 37 °C.

RESULTS AND DISCUSSION

Apocytochrome b_5 was overexpressed, uniformly enriched with ^{15}N, and observed inside living *E. coli*. Figure 2A shows the in-cell ^{1}H−^{15}N HSQC spectrum. The ^{1}H−^{15}N HSQC spectrum of purified, ^{15}N-enriched apocytochrome b_5 in dilute solution [0.5 mM apocytochrome b_5 and 50 mM phosphate buffer (pH 7.0)] is shown in Figure 2B. Each HSQC cross-peak arises from the covalent bond between an amide ^{15}N and its proton. Cross-peaks associated with the holoprotein were not observed in either spectrum.

Additional cross-peaks can be seen in the in-cell HSQC spectrum (Figure 2A) compared to the dilute solution spectrum (Figure 2B). Several of these cross-peaks are circled in Figure 2A. To identify the source of these cross-peaks, we acquired an in-cell ^{1}H−^{15}N HSQC spectrum of *E. coli* strain BL21(DE3) Gold without the pET3d(*cytb5*) plasmid. This spectrum is shown in Figure 3. Comparing Figures 2A and 3 shows that the extra cross-peaks arise from metabolites that have incorpated ^{15}N from the growth medium. Although none of the extra cross-peaks have been firmly assigned to specific molecules, the ^{15}N-enriched metabolites probably include the enterobacterial common antigen (*21*) and other common compounds known to exist in the *E. coli* cytosol (*22*). This background noise, produced by the *E. coli* system grown in ^{15}N-enriched medium, must be overcome with overexpression of the protein being studied. These additional cross-peaks posed no problem in the analysis of apocytochrome b_5 using in-cell NMR.

The pattern of protein cross-peaks is a fingerprint of the backbone structure. Cross-peaks from the in-cell and dilute solution spectra were assigned on the basis of the dilute solution assignments at pH 6.2 and 7.7 (*8*, *15*). Only 92 of a possible 95 cross-peaks were assigned because of the overlap of cross-peaks for Ala4, Ser64, and Glu92 (*8*, *15*). Cross-peaks for Ser18 and Ser85 are not visible in Figure 2B because of their lower intensity. These cross-peaks are observed at lower contour levels as shown in the box (even at the lower contour level, we were unable to locate the cross-peak for Ala54 in the dilute solution spectrum). Two controls prove that the apocytochrome b_5 is inside living cells. First, ~90% of the cells are alive after a 48 h in-cell NMR

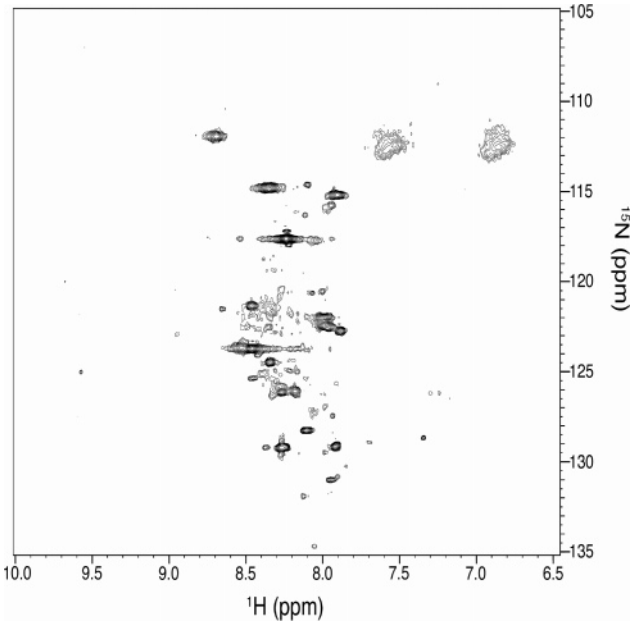

FIGURE 3: ^{1}H−^{15}N HSQC spectrum of *E. coli* lacking the expression system for apocytochrome b_5 grown in ^{15}N-enriched media. Cross-peaks belong to ^{15}N-enriched metabolites that accumulated during cellular growth.

experiment. Second, more than 90% of the protein is located in the soluble cytoplasmic fraction of the cells.

The lack of cross-peak broadening in the in-cell spectrum compared to the dilute solution spectrum indicates that apocytochrome b_5 is a monomer and is not tightly associated with any large molecules. Most importantly, there is no significant difference in cross-peak locations between the in-cell and dilute solution spectra, indicating no large changes in structure between the two environments. This congruence of chemical shifts also shows that the crowded environment does not induce native structure in the heme-binding region.

Apocytochrome b_5 backbone dynamics were quantified by measuring steady-state {^{1}H}−^{15}N nOes. The in-cell experiment was performed once on each of three different samples. The in vitro experiment was performed three times on one sample under dilute solution conditions. The averaged ratio of peak intensities (with ^{1}H saturation divided by without ^{1}H saturation) was used to quantify the nOe for each resolved cross-peak. The in-cell and in vitro experiments produced nOe values for 68 and 67 residues, respectively. Values for the 59 common residues were determined under both conditions (Figure 4).

For proteins the size of apocytochrome b_5, rigid backbone regions give nOe values of ~0.8 (at a ^{1}H frequency of 700 MHz). Less rigid regions give smaller values, and highly dynamic regions exhibit negative nOe values. These different regions can be seen in Figure 4. The in-cell data and the dilute solution data exhibit similar trends; the helices and sheets of the structured regions (Asp3−Glu38 and Leu70−Ser85) tend toward rigidity, while the heme-binding loop (His39−Glu69) and the termini are the most dynamic.

Changes in {^{1}H}−^{15}N nOe values between inside cells and dilute solution are mapped onto the structure in Figure 1. Differences in nOe values greater than the sum of their standard errors were deemed significant. Consequently, of the nOes for the 59 common residues, 18 are similar in cells and in dilute solution, 34 have smaller nOes in cells, and six have larger nOes in cells. There is no obvious correlation between the changes in nOe and the structure of apocytochrome b_5.

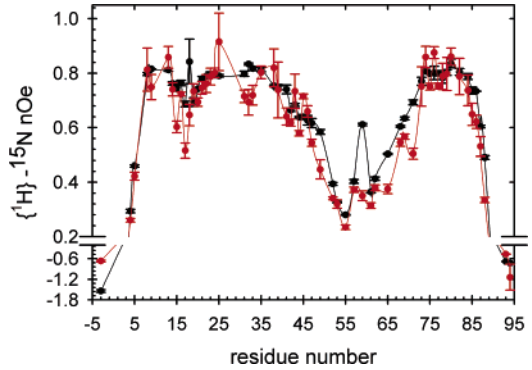

FIGURE 4: Steady-state {^{1}H}−^{15}N nOe values (700 MHz) quantified inside cells (red) and in dilute solution (black). Points are the averages of three measurements. Vertical bars indicate one standard error. The sequence numbering system is based on the sequence of bovine cytochrome b_5.

Although it is tempting to interpret the small decreases in intracellular nOes as increases in fast dynamics, we also must consider the effect of viscosity on nOe data. The viscosity of the *E. coli* cytoplasm is estimated to be 1.2−1.5-fold higher than the viscosity of a dilute buffer solution (*23*). We tested the idea that viscosity affects the results using two approaches. First, we mimicked the effect of this increased viscosity by using the dilute solution ^{15}N relaxation data (*8*), the appropriate equations describing the steady-state {^{1}H}−^{15}N nOe (*2*, *24*, *25*), and the Stokes−Einstein equation to calculate the effects on {^{1}H}−^{15}N nOes. We found that decreased nOes are expected for amides with slow internal correlation times such as those found throughout apocytochrome b_5 (*8*). The results of these simulations were confirmed by the second approach in which we quantified the {^{1}H}−^{15}N nOes for yeast isoferricytochrome *c* in vitro in dilute solution and in the presence of the viscogen glucose (G. J. Pielak, unpublished results). The results indicate that the residue positions showing decreased nOes in 1 M glucose are those that are known to have slow internal correlation times in dilute solution (*26*). However, the increased nOes observed in cells may represent small increases in rigidity inside cells, but we cannot rule out the effect of viscosity on residues with fast internal correlations. Whatever their source, it is important to avoid overinterpretation of the small observed changes in {^{1}H}−^{15}N nOes observed in cells and in the glucose experiments because both small and large molecule crowding agents are known to increase the structural stability of proteins (*7*, *27*). This influence of crowding agents on stability makes it difficult to conclude that the changes in dynamics observed in cells and in 1 M glucose are due solely to the changes in viscosity.

It is important to bear in mind that we chose an extremely simple protein for this initial study. Except for the heme moiety, which cannot be synthesized fast enough by the bacteria to yield a significant concentration of the holoprotein, apocytochrome b_5 does not appear to interact strongly with any molecules, large or small, inside *E. coli*. Many other proteins, however, do have specific interactions with other proteins, small molecule ligands, nucleic acids, or membranes. Such interactions are known to affect protein dynamics in vitro (*28*). It should be possible to study such

ligand-induced dynamic changes in more complicated protein systems by using in-cell NMR.

In summary, we have shown that quantitative information describing protein backbone dynamics can be obtained inside living cells. Even though some of the nOe values differ between dilute solution and inside cells, most of the differences track the change in viscosity rather than a change in fast backbone dynamics. Therefore, it appears that dilute solution steady-state $\{^1H\}-^{15}N$ nOe measurements can provide biologically relevant information about pico- to nanosecond backbone motion for simple protein systems such as the one studied here. Studies are underway to assess slower motions.

ACKNOWLEDGMENT

We thank the members of the Pielak laboratory, Elizabeth Pielak, and Matthew Redinbo for helpful discussions. We thank Jillian Orans for help with Figure 1 and Nancy Scott for plasmid preparation.

REFERENCES

1. Lindorff-Larsen, K., Best, R. B., Depristo, M. A., Dobson, C. M., and Vendruscolo, M. (2005) Simultaneous determination of protein structure and dynamics, *Nature 433*, 128−132.
2. Kay, L. E., Torchia, D. A., and Bax, A. (1989) Backbone dynamics of proteins as studied by ^{15}N inverse detected heteronuclear NMR spectroscopy: Application to staphylococcal nuclease, *Biochemistry 28*, 8972−8979.
3. Luby-Phelps, K. (2000) Cytoarchitecture and physical properties of cytoplasm: Volume, viscosity, diffusion, intracellular surface area, *Int. Rev. Cytol. 192*, 189−221.
4. Rivas, G., Fernandez, J. A., and Minton, A. P. (2001) Direct observation of the enhancement of noncooperative protein self-assembly by macromolecular crowding: Indefinite linear self-association of bacterial cell division protein FtsZ, *Proc. Natl. Acad. Sci. U.S.A. 98*, 3150−3155.
5. Dedmon, M. M., Patel, C. N., Young, G. B., and Pielak, G. J. (2002) FlgM gains structure in living cells, *Proc. Natl. Acad. Sci. U.S.A. 99*, 12681−12684.
6. Hatters, D. M., Minton, A. P., and Howlett, G. J. (2002) Macromolecular crowding accelerates amyloid formation by human apolipoprotein C-II, *J. Biol. Chem. 277*, 7824−7830.
7. Sasahara, K., McPhie, P., and Minton, A. P. (2003) Effect of dextran on protein stability and conformation attributed to macromolecular crowding, *J. Mol. Biol. 326*, 1227−1237.
8. Bhattacharya, S., Falzone, C. J., and Lecomte, J. T. (1999) Backbone dynamics of apocytochrome b_5 in its native, partially folded state, *Biochemistry 38*, 2577−2589.
9. Falzone, C. J., Wang, Y., Vu, B. C., Scott, N. L., Bhattacharya, S., and Lecomte, J. T. (2001) Structural and dynamic perturbations induced by heme binding in cytochrome b_5, *Biochemistry 40*, 4879−4891.
10. Serber, Z., Keatinge-Clay, A. T., Ledwidge, R., Kelly, A. E., Miller, S. M., and Dötsch, V. (2001) High-resolution macromolecular NMR spectroscopy inside living cells, *J. Am. Chem. Soc. 123*, 2446−2447.
11. Hubbard, J. A., MacLachlan, L. K., King, G. W., Jones, J. J., and Fosberry, A. P. (2003) Nuclear magnetic resonance spectroscopy reveals the functional state of the signaling protein CheY *in vivo* in *Escherichia coli*, *Mol. Microbiol. 49*, 1191−1200.
12. Serber, Z., and Dötsch, V. (2001) In-cell NMR spectroscopy, *Biochemistry 40*, 14317−14323.
13. Serber, Z., Straub, W., Corsini, L., Nomura, A. M., Shimba, N., Craik, C. S., de Montellano, P. O., and Dötsch, V. (2004) Methyl groups as probes for proteins and complexes in in-cell NMR experiments, *J. Am. Chem. Soc. 126*, 7119−7125.
14. Shimba, N., Serber, Z., Ledwidge, R., Miller, S. M., Craik, C. S., and Dötsch, V. (2003) Quantitative identification of the protonation state of histidines *in vitro* and *in vivo*, *Biochemistry 42*, 9227−9234.
15. Falzone, C. J., Mayer, M. R., Whiteman, E. L., Moore, C. D., and Lecomte, J. T. (1996) Design challenges for hemoproteins: The solution structure of apocytochrome b_5, *Biochemistry 35*, 6519−6526.
16. Delaglio, F., Grzesiek, S., Vuister, G. W., Zhu, G., Pfeifer, J., and Bax, A. (1995) NMRPipe: A multidimensional spectral processing system based on UNIX pipes, *J. Biomol. NMR 6*, 277−293.
17. Bodenhausen, G., and Ruben, D. J. (1980) Natural abundance nitrogen-15 NMR by enhanced heteronuclear spectroscopy, *Chem. Phys. Lett. 69*, 185−189.
18. Kay, L. E., Keifer, P., and Saarinen, T. (1992) Pure absorption gradient enhanced heteronuclear single quantum correlation spectroscopy with improved sensitivity, *J. Am. Chem. Soc. 114*, 10663−10665.
19. Farrow, N. A., Muhandiram, R., Singer, A. U., Pascal, S. M., Kay, C. M., Gish, G., Shoelson, S. E., Pawson, T., Forman-Kay, J. D., and Kay, L. E. (1994) Backbone dynamics of a free and phosphopeptide-complexed Src homology 2 domain studied by ^{15}N relaxation, *Biochemistry 33*, 5984−6003.
20. Lee, A. L., and Wand, A. J. (1999) Assessing potential bias in the determination of rotational correlation times of proteins by NMR relaxation, *J. Biomol. NMR 13*, 101−112.
21. Erbel, P. J. A., Seidel, R., Macintosh, S. E., Gentile, L. N., Amor, J. C., Kahn, R. A., Prestegard, J. H., McIntosh, L. P., and Gardner, K. H. (2004) Cyclic enterobacterial common antigen: Potential contaminant of bacterially expressed protein preparations, *J. Biomol. NMR 29*, 199−204.
22. Nobeli, I., Ponstingl, H., Krissinel, E. B., and Thornton, J. M. (2003) A structure-based anatomy of the *E. coli* metabolome, *J. Mol. Biol. 334*, 697−719.
23. Bicknese, S., Periasamy, N., Shohet, S. B., and Verkman, A. S. (1993) Cytoplasmic viscosity near the cell plasma membrane: Measurement by evanescent field frequency-domain microfluorimetry, *Biophys. J. 65*, 1272−1282.
24. Lipari, G., and Szabo, A. (1982) Model-free approach to the interpretation of nuclear magnetic resonance-relaxation in macromolecules. 1. Theory and range of validity, *J. Am. Chem. Soc. 104*, 4546−4559.
25. Lipari, G., and Szabo, A. (1982) Model-free approach to the interpretation of nuclear magnetic resonance-relaxation in macromolecules. 2. Analysis of experimental results, *J. Am. Chem. Soc. 104*, 4559−4570.
26. Fetrow, J. S., and Baxter, S. M. (1999) Assignment of ^{15}N chemical shifts and ^{15}N relaxation measurements for oxidized and reduced iso-1-cytochrome *c*, *Biochemistry 38*, 4480−4492.
27. Davis-Searles, P. R., Saunders, A. J., Erie, D. A., Winzor, D. J., and Pielak, G. J. (2001) Interpreting the effects of small uncharged solutes on protein-folding equilibria, *Annu. Rev. Biophys. Biomol. Struct. 30*, 271−306.
28. Ishima, R., and Torchia, D. A. (2000) Protein dynamics from NMR, *Nat. Struct. Biol. 7*, 740−743.

BI050786J